

Continuous contact problem of a functionally graded layer resting on an elastic half-plane

E. ÖNER¹⁾, G. ADIYAMAN²⁾, A. BIRINCI²⁾

¹⁾*Department of Civil Engineering
Bayburt University
69000 Bayburt, Turkey
e-mail: eoner@bayburt.edu.tr*

²⁾*Department of Civil Engineering
Karadeniz Technical University
61080 Trabzon, Turkey
e-mails: gadiyaman@ktu.edu.tr, birinci@ktu.edu.tr*

IN THIS STUDY, THE CONTINUOUS CONTACT PROBLEM of a functionally graded layer resting on an elastic half-plane and loaded by a rigid rectangular stamp is examined. The problem is solved assuming that the functionally graded (FG) layer is isotropic and the shear modulus and mass density vary exponentially throughout the layer's thickness. However, the body force of the elastic half-plane is neglected. In addition, it is assumed that all surfaces are frictionless and only compressive stress is transferred along the contact surfaces. The mathematical problem is reduced to a singular integral equation in which the contact stress under the rigid stamp is unknown using the Fourier integral transform and boundary conditions related to the problem. This singular integral equation is solved numerically using the Gauss–Chebyshev integration formula. The dimensionless contact stress under the rigid stamp, the initial separation loads and the initial separation distances between the FG layer and the elastic half-plane are obtained for various dimensionless quantities.

Key words: functionally graded layer, contact problem, initial separation load, initial separation distance, singular integral equation.

Copyright © 2017 by IPPT PAN

1. Introduction

WITH THE ADVANCEMENTS IN MATERIALS SCIENCE, the production methods in which material properties can be continuously varied along the thickness of material have been developed. The materials produced using such methods are generally referred to as functionally graded materials (FGMs). These materials are used in various applications, including ball and roller bearings, gears, cutting edges, gas turbines, electromagnetic engineering and space vehicles, mostly to provide abrasion resistance and high-temperature endurance. Such a wide range of application has resulted in the inevitable use of FGMs in contact me-

chanics. Several studies have examined the contact problems of layers made from FGMs.

GIANNAKOPOULOS and PALLOT [1] examined two-dimensional contact of a rigid cylinder on an elastic graded substrate. GULER AND ERDOGAN [2, 3] studied the fracture initiation in graded coatings under sliding contact loading and the contact problem for two deformable solids with FGM coatings. A receding contact plane problem between a functionally graded layer and a homogeneous substrate was considered by EL BORGI *et al.* [4]. A multi-layered model for frictionless contact analysis of functionally graded materials (FGMs) with arbitrarily varying elastic modulus under plane strain-state deformation was developed by KE and WANG [5]. GULER and ERDOGAN [6] examined the contact problems of parabolic and cylindrical stamps on graded coatings. A two-dimensional sliding frictional contact of functionally graded materials was studied by KE and WANG [7]. YANG and KE [8] investigated the two-dimensional frictionless contact problem of a coating structure consisting of a surface coating, a functionally graded layer and a substrate under a rigid cylindrical punch. The problem of a functionally graded coated half-space indented by an axisymmetric smooth rigid punch was studied by LIU and WANG [9]. A new method to solve the axisymmetric frictionless contact problem of functionally graded materials (FGMs) was examined by LIU *et al.* [10]. RHIMI *et al.* [11] considered a receding contact axisymmetric problem between a functionally graded layer and a homogeneous substrate. DAG *et al.* [12] studied the sliding frictional contact between a rigid punch and a laterally graded elastic medium. KE *et al.* [13] considered the sliding frictional contact problem of a layered half-plane made of functionally graded piezoelectric materials (FGPMs) in the plane strain state. The axisymmetric problem of a frictionless double receding contact between a rigid stamp of axisymmetric profile, an elastic functionally graded layer and a homogeneous half space was investigated by RHIMI *et al.* [14]. A theoretical analysis of two-dimensional frictionless sliding contact over orthotropic piezoelectric materials indented by a rigid sliding punch was carried out by ZHOU and LEE [15]. The contact problem for a functionally graded layer supported by a Winkler foundation was examined by COMEZ [16]. VOLKOV *et al.* [17] studied analytical solution of axisymmetric contact problem of indentation of a circular indenter into a soft, functionally graded elastic layer. The problem of sliding frictional contact between a laterally graded elastic medium and a rigid circular stamp was considered by DAG *et al.* [18]. LIU and XING [19] examined the contact-damage resistance of functionally graded materials coating. Elastic contact of a functionally graded plate of finite dimensions with continuous variation of material properties and a rigid spherical indenter was studied by NIKBAKHT *et al.* [20]. A frictional receding contact plane problem between a functionally graded layer and a homogeneous substrate was studied by

EL BORGI *et al.* [21]. VASILIEV *et al.* [22] studied axisymmetric contact problems of the theory of elasticity for inhomogeneous layers. YAN and LI [23] considered a double receding contact plane problem between a functionally graded layer and an elastic layer. COMEZ [24] solved a contact problem for a functionally graded layer indented by a moving punch. Axisymmetric contact problem on the indentation of a hot circular punch into an arbitrarily nonhomogeneous half-space was considered by KRENEV *et al.* [25]. WANG *et al.* [26] investigated an efficient method for solving three-dimensional fretting contact problems involving multilayered or functionally graded materials. A three-dimensional problem of elasticity of normal and tangential loading of surface of the functionally graded coated half-space was examined by KULCHYTSKY-ZHYHAILO and BAJKOWSKI [27]. MA *et al.* [28] investigated a frictional contact problem between a functionally graded magneto-electro-elastic layer and a rigid conducting flat punch with frictional heat generation. ALINIA *et al.* [29] considered the fully coupled contact problem between a rigid cylinder and a functionally graded coating bonded to a homogeneous substrate system under plane strain and generalized plane stress sliding conditions. Frictional receding contact analysis of a layer on a half-plane subjected to semi-infinite surface pressure was studied by PAREL and HILLS [30].

An examination of the related literature shows that although many studies have investigated the contact of FG layers, the body force of FG layer has been neglected. Therefore, this study aims to solve the continuous contact problem of an FG layer resting on an elastic half-plane by taking into account the body force of an FG layer. However, the body force of the elastic half-plane is neglected. Furthermore, the calculations are made under the assumption that the FG layer is isotropic and the shear modulus and mass density exponentially vary along the direction of the layer's thickness.

2. Formulation of the continuous contact problem

2.1. The case with body forces neglected

As shown in Fig. 1, an infinite FG layer with a thickness h and loaded by a rigid rectangular stamp is in smooth contact with a homogeneous half-plane. It is assumed that the FG layer is inhomogeneous and isotropic. In addition, the shear modulus μ_1 of the FG layer is modelled using an exponential function and depends only on the y -coordinate. Consequently, μ_1 can be expressed as follows:

$$(2.1) \quad \mu_1(y) = \mu_0 e^{\beta y} \quad (-h < y \leq 0),$$

where μ_0 is the shear modulus of the FG layer at $y = 0$ and β is an arbitrary non-zero constant that characterizes the material's inhomogeneity.

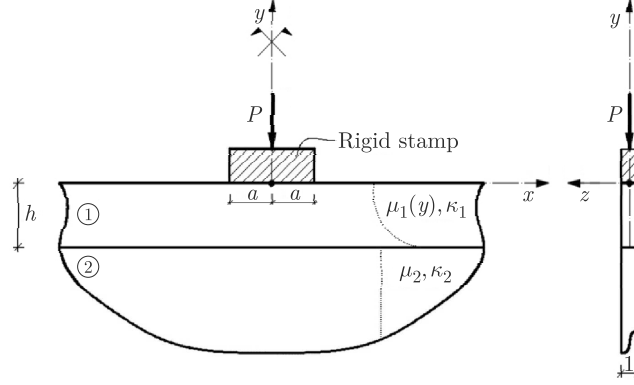


FIG. 1. Geometry and loading condition of the continuous contact problem.

The equilibrium equations with the body forces neglected and with the linear elastic stress-strain expressions can be written respectively as

$$(2.2) \quad \frac{\partial \sigma_x}{\partial x} + \frac{\tau_{xy}}{\partial y} = 0,$$

$$(2.3) \quad \frac{\partial \tau_{xy}}{\partial x} + \frac{\partial \sigma_y}{\partial y} = 0,$$

$$(2.4) \quad \sigma_x = \frac{\mu_j}{\kappa_j - 1} \left[(1 + \kappa_j) \frac{\partial u}{\partial x} + (3 - \kappa_j) \frac{\partial v}{\partial y} \right] \quad (j = 1, 2),$$

$$(2.5) \quad \sigma_y = \frac{\mu_j}{\kappa_j - 1} \left[(3 - \kappa_j) \frac{\partial u}{\partial x} + (1 + \kappa_j) \frac{\partial v}{\partial y} \right] \quad (j = 1, 2),$$

$$(2.6) \quad \tau_{xy} = \mu_j \left(\frac{\partial u}{\partial y} + \frac{\partial v}{\partial x} \right) \quad (j = 1, 2),$$

where u and v indicate the displacement components in the x and y directions, respectively, σ_x , σ_y and τ_{xy} denote the components of the stress field, ε_{xx} , ε_{yy} and ε_{xy} are defined as the corresponding components of the strain field, κ_j is Kolosov's constant and $\kappa_j = 3 - 4\nu_j$ ($j = 1, 2$) for the plane strain problem and ν_j ($j = 1, 2$) is Poisson's ratio.

By substituting the linear elastic stress-strain expressions of Eqs. (2.4)–(2.6) into the equilibrium equations (Eqs. (2.2)–(2.3)), the two-dimensional Navier equations can be obtained for the FG layer as

$$(2.7) \quad (\kappa_1 + 1) \frac{\partial^2 u}{\partial x^2} + (\kappa_1 - 1) \frac{\partial^2 u}{\partial y^2} + 2 \frac{\partial^2 v}{\partial x \partial y} + \beta(\kappa_1 - 1) \frac{\partial u}{\partial y} + \beta(\kappa_1 - 1) \frac{\partial v}{\partial x} = 0$$

$$(-h < y \leq 0),$$

$$(2.8) \quad (\kappa_1 - 1) \frac{\partial^2 v}{\partial x^2} + (\kappa_1 + 1) \frac{\partial^2 v}{\partial y^2} + 2 \frac{\partial^2 u}{\partial x \partial y} + \beta(3 - \kappa_1) \frac{\partial u}{\partial x} + \beta(\kappa_1 + 1) \frac{\partial v}{\partial y} = 0$$

$$(-h < y \leq 0),$$

and for the elastic half-plane as

$$(2.9) \quad (\kappa_2 + 1) \frac{\partial^2 u}{\partial x^2} + (\kappa_2 - 1) \frac{\partial^2 u}{\partial y^2} + 2 \frac{\partial^2 v}{\partial x \partial y} = 0 \quad (y \leq -h),$$

$$(2.10) \quad (\kappa_2 - 1) \frac{\partial^2 v}{\partial x^2} + (\kappa_2 + 1) \frac{\partial^2 v}{\partial y^2} + 2 \frac{\partial^2 u}{\partial x \partial y} = 0 \quad (y \leq -h).$$

To solve Eqs. (2.7)–(2.8), the Fourier sine and cosine transforms are applied to the variable x . The transform pairs for the displacements are defined as

$$(2.11) \quad u(x, y) = \frac{2}{\pi} \int_0^{\infty} \varphi(\xi, y) \sin(\xi x) d\xi,$$

$$v(x, y) = \frac{2}{\pi} \int_0^{\infty} \psi(\xi, y) \cos(\xi x) d\xi,$$

$$(2.12) \quad \varphi(\xi, y) = \int_0^{\infty} u(x, y) \sin(\xi x) dx,$$

$$\psi(\xi, y) = \int_0^{\infty} v(x, y) \cos(\xi x) dx,$$

where $\varphi(\xi, y)$ and $\psi(\xi, y)$ are converted from $u(x, y)$ and $v(x, y)$, respectively, using the Fourier sine and cosine transforms and ξ represents the transform variable. Applying the Fourier sine and cosine transforms given in Eq. (2.12) to Eqs. (2.7)–(2.8) and solving the resulting system of homogeneous ordinary differential equations, the following expressions are obtained:

$$(2.13) \quad \varphi(y) = \sum_{j=1}^4 A_j e^{n_j y}, \quad (-h < y \leq 0),$$

$$(2.14) \quad \psi(y) = \sum_{j=1}^4 A_j m_j e^{n_j y} \quad (-h < y \leq 0),$$

where A_j ($j = 1, 2, 3, 4$) are the unknown functions that will be determined from the boundary conditions of the problem and n_j ($j = 1, \dots, 4$) are the roots of the following characteristic equation:

$$(2.15) \quad n_j^4 + 2\beta n_j^3 + (\beta^2 - 2\xi^2)n_j^2 - 2\xi^2\beta n_j + \xi^2 \left(\xi^2 + \beta^2 \frac{3 - \kappa_1}{\kappa_1 + 1} \right) = 0.$$

The roots n_j ($j = 1, \dots, 4$) can be obtained as

$$(2.16) \quad n_1 = -\frac{1}{2} \left(\beta + \sqrt{4\xi^2 + \beta^2 - 4\xi\beta i \sqrt{\frac{3 - \kappa_1}{\kappa_1 + 1}}} \right),$$

$$n_2 = -\frac{1}{2} \left(\beta - \sqrt{4\xi^2 + \beta^2 - 4\xi\beta i \sqrt{\frac{3 - \kappa_1}{\kappa_1 + 1}}} \right),$$

$$(2.17) \quad n_3 = -\frac{1}{2} \left(\beta + \sqrt{4\xi^2 + \beta^2 + 4\xi\beta i \sqrt{\frac{3 - \kappa_1}{\kappa_1 + 1}}} \right),$$

$$n_4 = -\frac{1}{2} \left(\beta - \sqrt{4\xi^2 + \beta^2 + 4\xi\beta i \sqrt{\frac{3 - \kappa_1}{\kappa_1 + 1}}} \right).$$

The known function m_j appearing in Eq. (2.14) can be expressed as

$$(2.18) \quad m_j = \frac{(3\beta + 2n_j - \beta\kappa_1)[n_j(\beta + n_j)(\kappa_1 + 1) - \xi^2(\kappa_1 + 3)]}{\xi[4\xi^2 - \beta^2(\kappa_1 - 3)(\kappa_1 + 1)]} \quad (j = 1, \dots, 4).$$

Substituting Eqs. (2.11) into Eqs. (2.4)–(2.6), the expressions of the stress field σ_y and τ_{xy} for the FG layer can be obtained as

$$(2.19) \quad \sigma_{1yh}(x, y) = \frac{2\mu_0 e^{\beta y}}{\pi(\kappa_1 - 1)} \int_0^\infty \sum_{j=1}^4 A_j C_j e^{n_j y} \cos(\xi x) d\xi \quad (-h < y \leq 0),$$

$$(2.20) \quad \tau_{1xyh}(x, y) = \frac{2\mu_0 e^{\beta y}}{\pi} \int_0^\infty \sum_{j=1}^4 A_j D_j e^{n_j y} \sin(\xi x) d\xi \quad (-h < y \leq 0),$$

where

$$(2.21) \quad C_j = (3 - \kappa_1)\xi + (\kappa_1 + 1)m_j n_j, \quad D_j = n_j - \xi m_j \quad (j = 1, \dots, 4).$$

For the elastic half-plane, Eqs. (2.9)–(2.10) are solved in a manner similar to that used for the FG layer. Therefore, the displacement field and the stress field with the body forces neglected are obtained as

$$(2.22) \quad v_{2h}(x, y) = \frac{2}{\pi} \int_0^\infty \left[\left[-B_1 + \left(\frac{\kappa_2}{\xi} - y \right) B_2 \right] e^{\xi y} \right] \cos(\xi x) d\xi,$$

$$(2.23) \quad \frac{1}{2\mu_2} \sigma_{2yh}(x, y) = \frac{2}{\pi} \int_0^\infty \left[\left[-\xi(B_1 + B_2 y) + \left(\frac{1 + \kappa_2}{2} \right) B_2 \right] e^{\xi y} \right] \cos(\xi x) d\xi,$$

$$(2.24) \quad \frac{1}{2\mu_2} \tau_{2xyh}(x, y) = \frac{2}{\pi} \int_0^{\infty} \left[\left[\xi(B_1 + B_2 y) + \left(\frac{1 - \kappa_2}{2} \right) B_2 \right] e^{\xi y} \right] \sin(\xi x) d\xi.$$

The subscripts h appearing in Eqs. (2.19)–(2.24) refer to the displacement and stress field for the FG layer and the elastic half-plane in the case when the body forces are neglected. Additionally, μ_2 and κ_2 are the shear modulus and the Kolosov constant respectively of the elastic half-plane.

2.2. The case including the body force of the FG layer

Consider an FG layer with a thickness h resting on an elastic half-plane, as shown in Fig. 2. Let $\rho_1(y)g$ be the body force acting vertically along the FG layer. Note that the body force acting on the elastic half-plane is neglected because it does not disturb the contact stress distribution. The mass density of the FG layer is assumed to vary exponentially throughout the thickness of the FG layer as

$$(2.25) \quad \rho_1(y) = \rho_0 e^{\gamma y},$$

where ρ_0 is the mass density of the FG layer at $y = 0$, γ is an arbitrary non-zero constant that characterizes the material's inhomogeneity and g is gravitational acceleration.

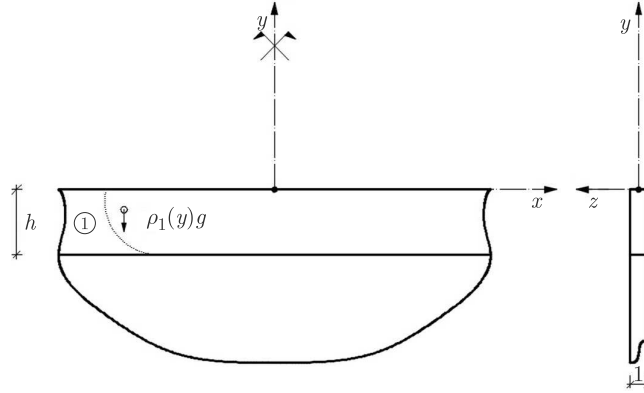


FIG. 2. Geometry of the problem relating to the case including the body force of the FG layer.

In the case where the body force of the FG layer is considered, the two-dimensional Navier equations can be written as

$$(2.26) \quad (\kappa_1 + 1) \frac{\partial^2 u}{\partial x^2} + (\kappa_1 - 1) \frac{\partial^2 u}{\partial y^2} + 2 \frac{\partial^2 v}{\partial x \partial y} + \beta(\kappa_1 - 1) \frac{\partial u}{\partial y} + \beta(\kappa_1 - 1) \frac{\partial v}{\partial x} = 0,$$

$$(2.27) \quad (\kappa_1 - 1) \frac{\partial^2 v}{\partial x^2} + (\kappa_1 + 1) \frac{\partial^2 v}{\partial y^2} + 2 \frac{\partial^2 u}{\partial x \partial y} + \beta(3 - \kappa_1) \frac{\partial u}{\partial x} + \beta(\kappa_1 + 1) \frac{\partial v}{\partial y} = \frac{\rho_0}{\mu_0} (\kappa_1 + 1) g e^{(\gamma - \beta)y},$$

where

$$(2.28) \quad u = u(x) \quad \text{and} \quad v = v(y).$$

If the rigid body displacement at the contact surface between the FG layer and the elastic half-plane is neglected, the boundary conditions in the case with a body force can be written as

$$(2.29) \quad u(0) = 0,$$

$$(2.30) \quad v(-h) = 0,$$

$$(2.31) \quad \sigma_y = \int_y^0 -\rho_0 e^{\gamma y} g dy,$$

$$(2.32) \quad \int_{-h}^0 \sigma_x dy = 0.$$

By solving Eqs. (2.26) and (2.27) and using the boundary conditions in Eqs. (2.29)–(2.32), the particular part of the stress field corresponding to the case with body force of the FG layer can be obtained as

$$(2.33) \quad \sigma_{1yp} = \frac{\rho_0 g (e^{\gamma y} - 1)}{\gamma}.$$

The subscripted p refers to the particular part of the stress and displacement fields corresponding to the existing body forces only. Then, the total stress field can be used to obtain the initial separation loads and distances for the FG layer:

$$(2.34) \quad \sigma_{1y}(x, y) = \frac{2\mu_0 e^{\beta y}}{\pi(\kappa_1 - 1)} \int_0^\infty \sum_{j=1}^4 A_j C_j e^{n_j y} \cos(\xi x) d\xi + \frac{\rho_0 g (e^{\gamma y} - 1)}{\gamma} \quad (-h < y \leq 0).$$

3. Boundary conditions of the problem and the singular integral equation

To determine the unknown constants A_j ($j = 1, \dots, 4$), the problem must be considered under the following boundary conditions and the global equilibrium

condition:

$$(3.1) \quad \tau_{1xy}(x, 0) = 0 \quad (0 \leq x < \infty),$$

$$(3.2) \quad \sigma_{1y} = \left\{ \begin{array}{l} -p(x) \\ 0 \end{array} \right\} \quad \left. \begin{array}{l} (0 \leq x < a) \\ (a \leq x < \infty) \end{array} \right\},$$

$$(3.3) \quad \tau_{1xy}(x, -h) = 0 \quad (0 \leq x < \infty),$$

$$(3.4) \quad \tau_{2xy}(x, -h) = 0 \quad (0 \leq x < \infty),$$

$$(3.5) \quad \sigma_{1y}(x, -h) = \sigma_{2y}(x, -h) \quad (0 \leq x < \infty),$$

$$(3.6) \quad \frac{\partial}{\partial x}[v_1(x, -h) - v_2(x, -h)] = 0 \quad (0 \leq x < \infty),$$

$$(3.7) \quad \frac{\partial}{\partial x}[v_1(x, 0)] = 0 \quad (0 \leq x < a).$$

By applying the boundary conditions in Eqs. (3.1)–(3.6) to the stress and displacement fields, the A_j ($j = 1, \dots, 4$) and B_i ($i = 1, 2$) coefficients can be determined in terms of the unknown contact stress $p(x)$. By substituting these coefficients into Eq. (3.7) and after some routine manipulations and the use of the symmetry condition $p(x) = p(-x)$, the following singular integral equation for $p(x)$ can be obtained:

$$(3.8) \quad \frac{1}{\pi} \int_{-a}^a \left[\frac{1}{t-x} + \frac{1}{h} k_1(x, t) \right] p(t) dt = 0 \quad (0 \leq x < a).$$

The kernel $k_1(x, t)$ is given by Eq. (A.1) in the Appendix. The equilibrium condition of the problem can be expressed as

$$(3.9) \quad \int_{-a}^a p(t) dt = P.$$

To obtain the initial separation load and initial separation distance between the FG layer and the elastic half-plane, the contact stress field $\sigma_{1y}(x, -h)$ needs to be determined. By substituting the values of A_j ($j = 1, \dots, 4$) as evaluated in terms of $p(x)$ into Eq. (2.34) and after some algebra manipulations, the contact stress field can be obtained as follows:

$$(3.10) \quad \sigma_{1y}(x, -h) = \frac{\rho_0 g (e^{-\gamma h} - 1)}{\gamma} - \frac{1}{\pi h} \int_{-a}^a k_2(x, t) p(t) dt \quad (0 \leq x < \infty).$$

The kernel $k_2(x, t)$ is given by Eq. (A.2) in the Appendix. To simplify the solution of the singular integral equation, the following dimensionless quantities are

introduced:

$$(3.11) \quad x = as, \quad t = ar, \quad g(r) = \frac{p(ar)}{\rho_0gh}.$$

Substituting the values from Eq. (3.11), Eqs. (3.8)–(3.10) can be obtained as follows:

$$(3.12) \quad \int_{-1}^1 \left[\frac{1}{r-s} + \frac{a}{h} k_1(s, r) \right] g(r) dr = 0 \quad (-1 < s < 1),$$

$$(3.13) \quad \frac{a}{h} \int_{-1}^1 g(r) dr = \frac{P}{\rho_0gh^2} = \lambda,$$

$$(3.14) \quad \frac{\sigma_{1y}(x, -h)}{\rho_0gh} = \frac{(e^{-\gamma h} - 1)}{\gamma h} - \frac{1}{\pi} \frac{a}{h} \int_{-1}^1 k_2(x, ar) g(r) dr,$$

where λ is defined as the load factor. Because the contact stress under a rigid stamp goes to infinity at the corners, i.e., $g(\pm 1) \rightarrow \infty$, the index of the singular integral equation (3.12) is +1. Assuming the solution of the integral equation as reported by ERGODAN and GUPTA in [31],

$$(3.15) \quad g(r) = \frac{G(r)}{\sqrt{(1-r^2)}} \quad (-1 < r < 1),$$

and using the appropriate Gauss–Chebyshev integration formula, Eqs. (3.12) and (3.13) can then be replaced by:

$$(3.16) \quad \sum_{i=1}^n W_i \left[\frac{1}{r_i - s_j} + \frac{a}{h} k_1(s_j, r_i) \right] G(r_i) = 0 \quad (j = 1, \dots, n-1),$$

$$(3.17) \quad \frac{a}{h} \sum_{i=1}^n W_i G(r_i) = \frac{\lambda}{\pi},$$

where

$$(3.18) \quad W_1 = W_n = \frac{1}{2n-2}, \quad W_i = \frac{1}{n-1} \quad (i = 2, \dots, n-1),$$

$$(3.19) \quad r_i = \cos\left(\frac{i-1}{n-1}\pi\right) \quad (i = 1, \dots, n),$$

$$(3.20) \quad s_j = \cos\left(\frac{2j-1}{n-1}\frac{\pi}{2}\right) \quad (j = 1, \dots, n-1).$$

Equations (3.16) and (3.17) constitute n linear algebraic equations for n unknowns, i.e., $G(r_i)$ ($i = 1, \dots, n$). The solution to these algebraic equations and the use of Eq. (3.15) yield the unknown contact stress function under the rigid stamp. Substituting the contact stress function into Eq. (3.14) and using the Gauss–Chebyshev integration formula, the contact stress $\sigma_{1y}(x, -h)$ between the FG layer and the elastic half-plane can be obtained.

In the case in which the λ load factor defined in Eq. (3.13) reaches a certain critical value (λ_{cr}), a separation occurs at the contact surface. Therefore, for Eq. (3.14) to be valid, the $\sigma_{1y}(x, -h)$ contact stress needs to be compressive at every point on the contact surface. This is only true if $0 \leq \lambda \leq \lambda_{cr}$. In the case in which $\lambda > \lambda_{cr}$, a separation occurs between the FG layer and the elastic half-plane and the problem turns into a discontinuous contact problem. Therefore, the boundary conditions for continuous contact are no longer valid.

To determine the initial separation load and initial separation distance between the FG layer and the elastic half-plane, Eq. (3.14) needs to be equalized to zero. Using this equation, the initial separation load and the initial separation distance (point) can be determined together. The critical load factor that causes the initial separation is given as follows:

$$(3.21) \quad \lambda_{cr} = \frac{P_{cr}}{\rho_0 g h^2}.$$

With load factors greater than critical load factor ($\lambda > \lambda_{cr}$), a separation begins to occur between the FG layer and the elastic half-plane, as stated above. In such a case, the problem needs to be addressed as a discontinuous contact problem.

4. Numerical results and discussion

In this study, the influence of the material inhomogeneity parameters βh and γh , the interface material property mismatch μ_{-h}/μ_2 and the rigid stamp width (a/h) on the dimensionless contact stress distribution under a rigid stamp was reported. In addition, the initial separation load λ_{cr} and the distance x_{cr}/h between the FG layer and the elastic half-plane were obtained for various values of material inhomogeneity parameters (βh and γh) and rigid stamp width (a/h). The shear modulus and mass density of the FG layer at $y = -h$, μ_{-h} and ρ_{-h} are defined as

$$(4.1) \quad \mu_{-h} = \mu_0 e^{-\beta h},$$

$$(4.2) \quad \rho_{-h} = \rho_0 e^{-\gamma h}.$$

As seen in Eqs. (4.1)–(4.2), $\beta h > 0$ and $\gamma h > 0$ indicate that the rigidity of the top surface of the layer is greater than that of the bottom surface, $\beta h = 0.001$

and $\gamma h = 0.0001$ correspond to a special case in which the layer is homogeneous and $\beta h < 0$ and $\gamma h < 0$ indicate that the rigidity of the top surface of the layer is lower than that of the bottom surface.

The contact stress distributions under rigid stamp ($y = 0$) for various dimensionless quantities such as a/h , βh and μ_{-h}/μ_2 are given in Figs. 3–5. Figure 3 illustrates how the stamp width (a/h) affects the dimensionless contact stress distribution under a rigid stamp. An examination of Fig. 3 suggests that the dimensionless contact stress decreases with an increasing stamp width. Figure 4 shows the effect of the inhomogeneity parameter βh on the dimensionless contact stress distribution under a rigid stamp. It is clear from the figure that as βh increases, i.e., as the rigidity of the layer decreases from top to bottom, the layer becomes softer and the dimensionless contact stress increases towards the edges of the stamp; however, the dimensionless contact stress decreases towards the mid-point of the stamp. The effect of the interface material property mismatch (μ_{-h}/μ_2) on the dimensionless contact stress distribution is shown in Fig. 5. It can be concluded from this figure that as (μ_{-h}/μ_2) increases, i.e., when the rigidity of bottom surface of the layer is greater than the rigidity of the elastic half-plane, the dimensionless contact stress increases toward the edges of the stamp whereas it decreases towards the mid-point of the stamp. In addition, Figs. 3–5 illustrate that the dimensionless contact stress becomes infinitely large

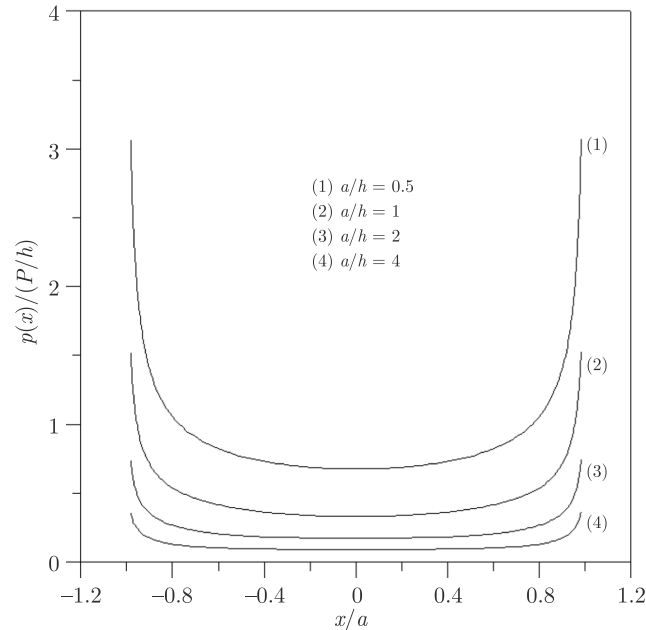


FIG. 3. Effect of the stamp width (a/h) on the dimensionless contact stress distribution under rigid stamp ($\kappa_1 = \kappa_2 = 2$, $\beta h = -0.6931$, $\mu_{-h}/\mu_2 = 1$, $h = 1$, $\mu_0 = 1$, $y = 0$).

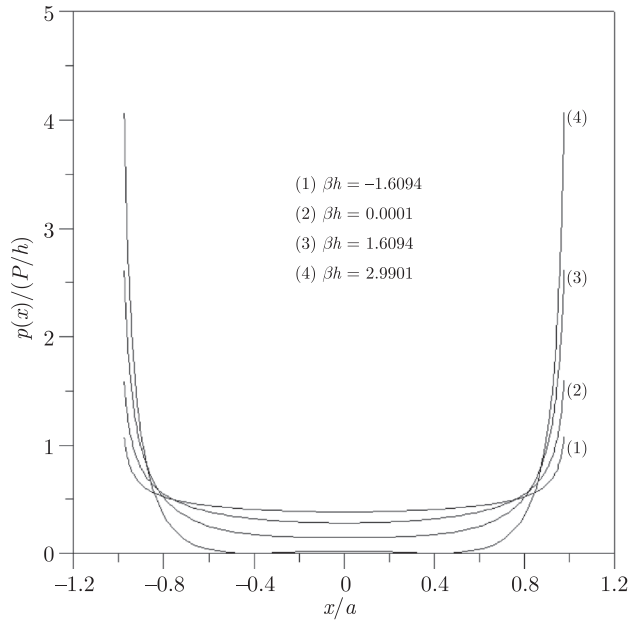


FIG. 4. Effect of the inhomogeneity parameter βh on the dimensionless contact stress distribution under rigid stamp ($\kappa_1 = \kappa_2 = 2$, $a/h = 1$, $\mu_{-h}/\mu_2 = 1$, $h = 1$, $\mu_0 = 1$, $y = 0$).

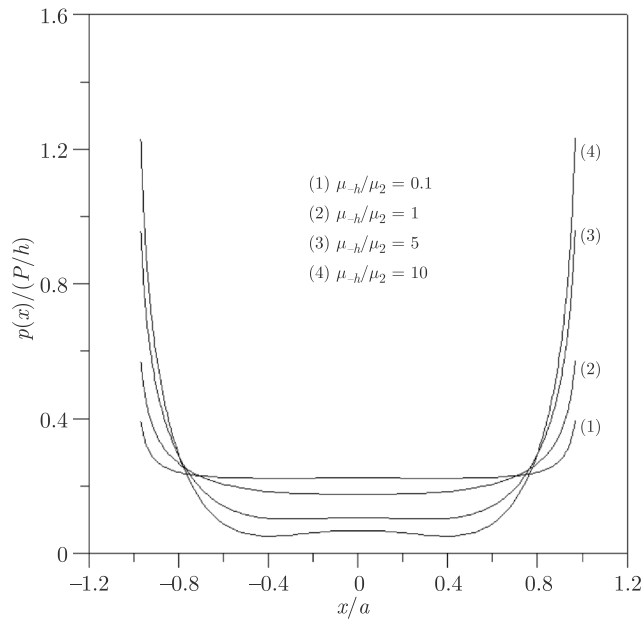


FIG. 5. The effect of interface material property mismatch (μ_{-h}/μ_2) on the dimensionless contact stress distribution under rigid stamp ($\kappa_1 = \kappa_2 = 2$, $a/h = 2$, $\beta h = -0.6931$, $h = 1$, $\mu_0 = 1$, $y = 0$).

at the edges of the rigid stamp and gradually decreases towards the $x = 0$ symmetry axis. This is an expected result because by examining the integral equation it can be shown that the edges of the rigid stamp are singular points for the stress.

In the case of a homogeneous layer ($\beta h = 0.001$ and $\gamma h = 0.0001$), one can compare the results with those obtained in CAKIROGLU [32], and for the same case, by assigning a large value to μ_2 ($\mu_2 \rightarrow \infty$), one can compare the results with those obtained in CIVELEK and ERDOGAN [33], and CIVELEK *et al.* [34]. The results of these comparisons are given in Tables 1 and 2, respectively. As listed in Tables 1 and 2, the initial separation loads and distances obtained for various stamp widths are very close to the results obtained in [32–34].

Table 1. Comparison of the initial separation loads and distances with those from CAKIROGLU [32] ($\kappa_1 = \kappa_2 = 2$, $y = -h$, $h = 1$, $\mu_0 = 1$, $\beta h = 0.001$, $\gamma h = 0.0001$).

(a/h) ↓	$\frac{(1 + \kappa_2) \mu_1}{(1 + \kappa_1) \mu_2} = 0.5$				$\frac{(1 + \kappa_2) \mu_1}{(1 + \kappa_1) \mu_2} = 1$			
	Present		Before [32]		Present		Before [32]	
	λ_{cr}	x_{cr}/h	λ_{cr}	x_{cr}/h	λ_{cr}	x_{cr}/h	λ_{cr}	x_{cr}/h
0.5	120.399	2.584	120.396	2.584	158.331	3.074	158.305	3.074
1	168.037	3.029	168.017	3.029	209.809	3.506	209.738	3.506
2	273.514	4.044	273.489	4.044	325.987	4.532	325.881	4.532
4	439.034	6.060	438.900	6.060	502.989	6.556	502.854	6.555

Table 2. Comparison of the initial separation loads and distances with those from CIVELEK and ERDOGAN [33], and CIVELEK *et al.* [34] ($\kappa_1 = \kappa_2 = 2$, $y = -h$, $h = 1$, $\mu_0 = 1$, $\beta h = 10^{-5}$, $\gamma h = 10^{-6}$).

(a/h) ↓	$\mu_2 \rightarrow \infty$			
	Present		Before [33, 34]	
	λ_{cr}	x_{cr}/h	λ_{cr}	x_{cr}/h
0.5	58.7965	2.00	58.78	–
1	92.3735	2.46	92.40	–
2	169.487	3.46	169.57	–
10^{-20}	44.13	1.77	44.13924	1.77055

The contact stress distributions between the FG layer and the elastic half-plane ($y = -h$) for various dimensionless quantities such as (a/h) , (βh) , (γh) and (μ_{-h}/μ_2) are given in Figs. 6–9. The effect of the stamp width (a/h) on the initial separation load and the distance is presented in Fig. 6. It can be concluded from this figure that with increasing values of the stamp width (a/h) , the initial separation loads and the initial separation distances increase. The effect of the

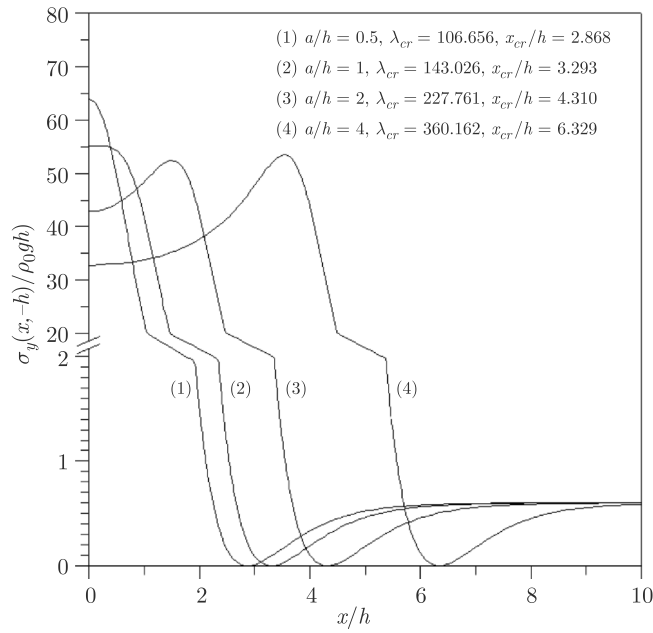


FIG. 6. The effect of stamp width (a/h) on the initial separation load and distance ($\kappa_1 = \kappa_2 = 2, \beta h = -0.6931, \gamma h = 1.0986, \mu_{-h}/\mu_2 = 1, h = 14, \mu_0 = 1, y = -h$).

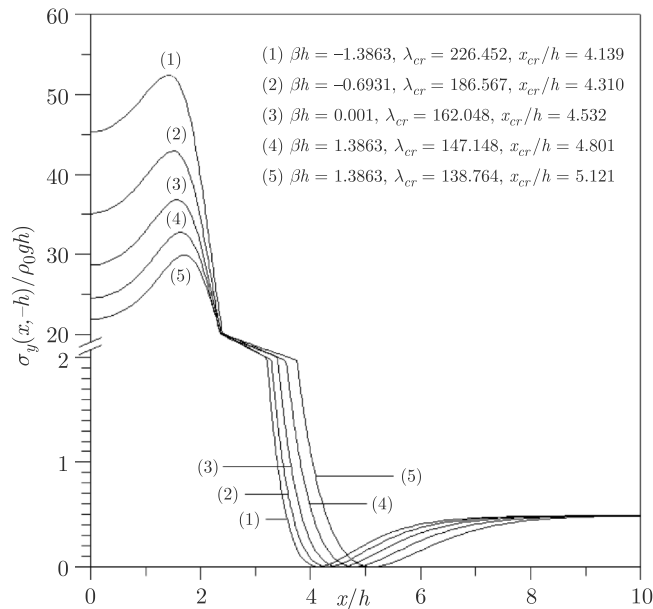


FIG. 7. Effect of the inhomogeneity parameter (βh) on the initial separation load and distance ($\kappa_1 = \kappa_2 = 2, a/h = 2, \gamma h = 1.6094, \mu_{-h}/\mu_2 = 1, h = 1, \mu_0 = 1, y = -h$).

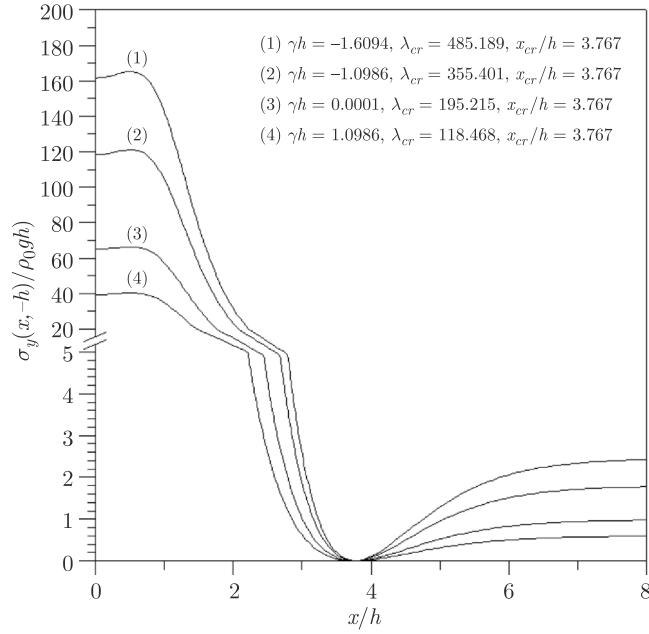


FIG. 8. Effect of the inhomogeneity parameter (γh) on the initial separation load and distance ($\kappa_1 = \kappa_2 = 2$, $a/h = 1$, $\beta h = 0.6931$, $\mu_{-h}/\mu_2 = 1$, $h = 1$, $\mu_0 = 1$, $y = -h$).

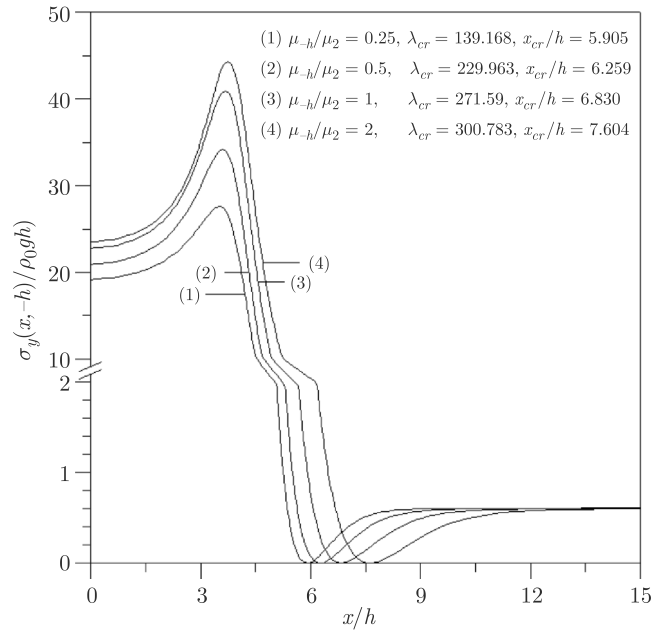


FIG. 9. The effect of interface material property mismatch (μ_{-h}/μ_2) on the initial separation load and distance ($\kappa_1 = \kappa_2 = 2$, $a/h = 4$, $\gamma h = 1.0986$, $\beta h = 0.6931$, $h = 1$, $\mu_0 = 1$, $y = -h$).

inhomogeneity parameters βh and γh on the initial separation load and the distance is presented in Figs. 7 and 8 and Table 3. An examination of Fig. 7 and Table 3 shows that with increasing values of βh , the initial separation loads decrease and the initial separation distances increase. Moreover, both Fig. 8 and Table 3 show a negative correlation between the inhomogeneity parameter γh and the initial separation load; however, the initial separation distance is not affected by the change in γh .

Table 3. Effect of the inhomogeneity parameters (βh) and (γh) on the initial separation loads and distance ($\kappa_1 = \kappa_2 = 2$, $a/h = 2$, $\mu_{-h}/\mu_2 = 1$, $h = 1$, $\mu_0 = 1$, $y = -h$).

(γh) ↓	βh									
	-1.3863		-0.6931		0.001		0.6931		1.3863	
	λ_{cr}	x_{cr}/h								
-1.6094	1132.22	4.139	932.799	4.310	810.209	4.532	735.714	4.801	693.795	5.121
-1.0986	829.348	4.139	683.274	4.310	593.477	4.532	538.91	4.801	508.204	5.121
0.0001	455.546	4.139	375.311	4.310	325.987	4.532	296.014	4.801	279.148	5.121
1.0986	276.453	4.139	227.761	4.310	197.828	4.532	179.639	4.801	169.403	5.121
1.6094	226.452	4.139	186.567	4.310	162.048	4.532	147.148	4.801	138.764	5.121

The effect of interface material property mismatch (μ_{-h}/μ_2) on the initial separation load and distance is shown in Fig. 9. As seen in this figure, the initial separation load and the initial separation distance increase with increasing values of (μ_{-h}/μ_2).

5. Conclusions

In this study, the continuous contact problem of the FG layer resting on the elastic half-plane was solved using the linear elasticity theory. The shear modulus and mass density of the layer were assumed to vary exponentially throughout the thickness of the layer. The dimensionless contact stress distribution under the stamp, initial separation loads and distances between the FG layer and the elastic half-plane were obtained for various values of stamp width (a/h), inhomogeneity parameters (βh and γh) and interface material property mismatch (μ_{-h}/μ_2). The dimensionless contact stress decreases with increasing stamp width. As the inhomogeneity parameter βh increases, the dimensionless contact stress increases towards the edges of the stamp and decreases towards the mid-point of the stamp. The same behaviour is observed in the case of increasing interface material property mismatch (μ_{-h}/μ_2). With increasing values of the inhomogeneity parameter βh , the initial separation loads decrease, whereas the initial separation distances increase. With increasing values of the non-homogeneity parameter γh , the initial separation loads decrease, whereas the initial separation distances remain

unchanged. With increasing values of the stamp width (a/h), the initial separation loads and the initial separation distances increase. As (μ_{-h}/μ_2) increases, the initial separation load and the initial separation distance increase.

Appendix

$$(A.1) \quad k_1(x, t) = \int_0^{\infty} \left\{ \begin{aligned} & ((4\xi(-4F\xi(D_3((e^{hn_1}-e^{hn_2})(e^{hn_3}-e^{hn_4})D_4m_1m_2 \\ & +((e^{hn_2}-e^{hn_3})(e^{hn_1}-e^{hn_4})D_2m_1-(e^{hn_1}-e^{hn_3})(e^{hn_2}-e^{hn_4})D_1m_2)m_4) \\ & -m_3(-(e^{hn_2}-e^{hn_3})(e^{hn_1}-e^{hn_4})D_1D_4m_2 \\ & +D_2((e^{hn_1}-e^{hn_3})(e^{hn_2}-e^{hn_4})D_4m_1-(e^{hn_1}-e^{hn_2})(e^{hn_3}-e^{hn_4})D_1m_4))) \\ & +C_4(-e^{hn_2}(e^{hn_1}-e^{hn_3})D_1D_3m_2+D_2(e^{hn_1}(e^{hn_2}-e^{hn_3})D_3m_1 \\ & +e^{hn_3}(e^{hn_1}-e^{hn_2})D_1m_3))(1+\kappa_2) \\ & -C_3(-e^{hn_2}(e^{hn_1}-e^{hn_4})D_1D_4m_2+D_2(e^{hn_1}(e^{hn_2}-e^{hn_4})D_4m_1 \\ & +e^{hn_4}(e^{hn_1}-e^{hn_2})D_1m_4))(1+\kappa_2) \\ & +C_2(-e^{hn_3}(e^{hn_1}-e^{hn_4})D_1D_4m_3+D_3(e^{hn_1}(e^{hn_3}-e^{hn_4})D_4m_1 \\ & +e^{hn_4}(e^{hn_1}-e^{hn_3})D_1m_4))(1+\kappa_2) \\ & -C_1(-e^{hn_3}(e^{hn_2}-e^{hn_4})D_2D_4m_3+D_3(e^{hn_2}(e^{hn_3}-e^{hn_4})D_4m_2 \\ & +e^{hn_4}(e^{hn_2}-e^{hn_3})D_2m_4))(1+\kappa_2))) / \Delta) - 1 \end{aligned} \right\} \times \sin(t-x) \frac{z}{h} dz$$

$$(A.2) \quad \Delta = (1+\kappa_1)(4e^{hn_4}F\xi C_4(-(e^{hn_1}-e^{hn_3})D_1D_3m_2 \\ + D_2((e^{hn_2}-e^{hn_3})D_3m_1+(e^{hn_1}-e^{hn_2})D_1m_3)) \\ + C_1(-4e^{hn_1}F\xi(-(e^{hn_2}-e^{hn_4})D_2D_4m_3 \\ + D_3((e^{hn_3}-e^{hn_4})D_4m_2+(e^{hn_2}-e^{hn_3})D_2m_4)) \\ + (e^{hn_2}-e^{hn_3})(e^{hn_1}-e^{hn_4})C_4D_2D_3(1+\kappa_2)) \\ + C_3(-4e^{hn_3}F\xi(-(e^{hn_1}-e^{hn_4})D_1D_4m_2 \\ + D_2((e^{hn_2}-e^{hn_4})D_4m_1+(e^{hn_1}-e^{hn_2})D_1m_4)) \\ + (e^{hn_1}-e^{hn_2})(e^{hn_3}-e^{hn_4})C_4D_1D_2(1+\kappa_2) \\ + (e^{hn_2}-e^{hn_3})(e^{hn_1}-e^{hn_4})C_2D_1D_4(1+\kappa_2) \\ - (e^{hn_1}-e^{hn_3})(e^{hn_2}-e^{hn_4})C_1D_2D_4(1+\kappa_2)) \\ + C_2(4e^{hn_2}F\xi(-(e^{hn_1}-e^{hn_4})D_1D_4m_3 \\ + D_3((e^{hn_3}-e^{hn_4})D_4m_1+(e^{hn_1}-e^{hn_3})D_1m_4)) \\ - (e^{hn_1}-e^{hn_3})(e^{hn_2}-e^{hn_4})C_4D_1D_3(1+\kappa_2) \\ + (e^{hn_1}-e^{hn_2})(e^{hn_3}-e^{hn_4})C_1D_3D_4(1+\kappa_2))),$$

$$(A.3) \quad k_2(x, t) = \int_0^{\infty} \left(\begin{aligned} &(-4e^{-h\beta} F\xi(C_4(-(e^{hn_1} - e^{hn_3})D_1D_3m_2 \\ &+ D_2((e^{hn_2} - e^{hn_3})D_3m_1 + (e^{hn_1} - e^{hn_2})D_1m_3)) \\ &- C_3(-(e^{hn_1} - e^{hn_4})D_1D_4m_2 + D_2((e^{hn_2} - e^{hn_4})D_4m_1 \\ &+ (e^{hn_1} - e^{hn_2})D_1m_4)) \\ &+ C_2(-(e^{hn_1} - e^{hn_4})D_1D_4m_3 + D_3((e^{hn_3} - e^{hn_4})D_4m_1 \\ &+ (e^{hn_1} - e^{hn_3})D_1m_4)) \\ &- C_1(-(e^{hn_2} - e^{hn_4})D_2D_4m_3 + D_3((e^{hn_3} - e^{hn_4})D_4m_2 \\ &+ (e^{hn_2} - e^{hn_3})D_2m_4))) \end{aligned} \right) / \Delta^* \times \cos(t-x) \frac{z}{h} dz,$$

$$(A.4) \quad \Delta^* = 4e^{hn_4} F\xi C_4(-(e^{hn_1} - e^{hn_3})D_1D_3m_2 \\ + D_2((e^{hn_2} - e^{hn_3})D_3m_1 + (e^{hn_1} - e^{hn_2})D_1m_3)) \\ + C_1(-4e^{hn_1} F\xi(-(e^{hn_2} - e^{hn_4})D_2D_4m_3 \\ + D_3((e^{hn_3} - e^{hn_4})D_4m_2 + (e^{hn_2} - e^{hn_3})D_2m_4)) \\ + (e^{hn_2} - e^{hn_3})(e^{hn_1} - e^{hn_4})C_4D_2D_3(1 + \kappa_2)) \\ + C_3(-4e^{hn_3} F\xi(-(e^{hn_1} - e^{hn_4})D_1D_4m_2 \\ + D_2((e^{hn_2} - e^{hn_4})D_4m_1 + (e^{hn_1} - e^{hn_2})D_1m_4)) \\ + (e^{hn_1} - e^{hn_2})(e^{hn_3} - e^{hn_4})C_4D_1D_2(1 + \kappa_2) \\ + (e^{hn_2} - e^{hn_3})(e^{hn_1} - e^{hn_4})C_2D_1D_4(1 + \kappa_2) \\ - (e^{hn_1} - e^{hn_3})(e^{hn_2} - e^{hn_4})C_1D_2D_4(1 + \kappa_2)) \\ + C_2(4e^{hn_2} F\xi(-(e^{hn_1} - e^{hn_4})D_1D_4m_3 \\ + D_3((e^{hn_3} - e^{hn_4})D_4m_1 + (e^{hn_1} - e^{hn_3})D_1m_4)) \\ - (e^{hn_1} - e^{hn_3})(e^{hn_2} - e^{hn_4})C_4D_1D_3(1 + \kappa_2) \\ + (e^{hn_1} - e^{hn_2})(e^{hn_3} - e^{hn_4})C_1D_3D_4(1 + \kappa_2)),$$

$$(A.5) \quad F = \frac{\mu_2(\kappa_1 - 1)}{\mu_0 e^{-\beta h}}.$$

References

1. A.E. GIANNAKOPOULOS, P. PALLOT, *Two-dimensional contact analysis of elastic graded materials*, J. Mech. Phys. Solids, **48**, 1597–1631, 2000.
2. M.A. GULER, F. ERDOGAN, *Contact mechanics of graded coatings*, Int. J. Solids Struct., **41**, 3865–3889, 2004.

3. M.A. GULER, F. ERDOGAN, *Contact mechanics of two deformable elastic solids with graded coatings*, Mech. Mater., **38**, 633–647, 2006.
4. S. EL-BORGI, R. ABDELMOULA, L. KEER, *A receding contact plane problem between a functionally graded layer and a homogeneous substrate*, Int. J. Solids Struct., **43**, 658–674, 2006.
5. L.L. KE, Y.S. WANG, *Two-dimensional contact mechanics of functionally graded materials with arbitrary spatial variations of material properties*, Int. J. Solids Struct., **43**, 5779–5798, 2006.
6. M.A. GULER, F. ERDOGAN, *The frictional sliding contact problems of rigid parabolic and cylindrical stamps on graded coatings*. Int. J. Mech. Sci., **49**, 161–182, 2007.
7. L.L. KE, Y.S. WANG, *Two-dimensional sliding frictional contact of functionally graded materials*, Eur. J. Mech. A/Solids, **26**, 171–188, 2007.
8. J. YANG, L.L. KE, *Two-dimensional contact problem for a coating-graded layer-substrate structure under a rigid cylindrical punch*, Int. J. Mech. Sci., **50**, 985–994, 2008.
9. T.J. LIU, Y.S. WANG, *Axisymmetric frictionless contact problem of a functionally graded coating with exponentially varying modulus*, Acta Mech., **199**, 151–165, 2008.
10. T.J. LIU, Y.S. WANG, C. ZHANG, *Axisymmetric frictionless contact of functionally graded materials*, Arch. Appl. Mech., **78**, 267–282, 2008.
11. M. RHIMI, S. EL-BORGI, W. BEN SAID, F. BEN JEMAA, *A receding contact axisymmetric problem between a functionally graded layer and a homogeneous substrate*, Int. J. Solids Struct., **46**, 3633–3642, 2009.
12. S. DAG, M.A. GULER, B. YILDIRIM, A.C. OZATAG, *Sliding frictional contact between a rigid punch and a laterally graded elastic medium*, Int. J. Solids Struct., **46**, 4038–4053, 2009.
13. L.L. KE, Y.S. WANG, J. YANG, S. KITIPORNCHAI, *Sliding frictional contact analysis of functionally graded piezoelectric layered half-plane*, Acta Mech., **209**, 249–268, 2010.
14. M. RHIMI, S. EL-BORGI, N. LAJNEF, *A double receding contact axisymmetric problem between a functionally graded layer and a homogeneous substrate*, Mech. Mater., **43**, 787–798, 2011.
15. Y.T. ZHOU, K.Y. LEE, *Exact solutions of a new 2D frictionless contact model for orthotropic piezoelectric materials indented by a rigid sliding punch*, Philos. Mag., **92**, 1937–1965, 2012.
16. I. COMEZ, *Contact problem of a functionally graded layer resting on a Winkler foundation*, Acta Mech., **224**, 2833–2843, 2013.
17. S. VOLKOV, A. AIZIKOVICH, Y.S. WANG, I. FEDOTOV, *Analytical solution of axisymmetric contact problem about indentation of a circular indenter into a soft functionally graded elastic layer*. Acta Mech. Sinica, **29**, 196–201, 2013.
18. S. DAG, M.A. GULER, B. YILDIRIM, A.C. OZATAG, *Frictional Hertzian contact between a laterally graded elastic medium and a rigid circular stamp*, Acta Mech., **224**, 1773–1789, 2013.
19. T.J. LIU, Y.M. XING, *Analysis of graded coatings for resistance to contact deformation and damage based on a new multi-layer model*, Int. J. Mech. Sci., **81**, 158–164, 2014.

20. A. NIKBAKHT, A.F. AREZOODAR, M. SADIGHI, A. TALEZADEH, *Analyzing contact problem between a functionally graded plate of finite dimensions and a rigid spherical indenter*, Eur. J. Mech. A/Solids, **47**, 92–100, 2014.
21. S. EL-BORGI, S. USMAN, M.A. GULER, *A frictional receding contact plane problem between a functionally graded layer and a homogeneous substrate*, Int. J. Solids Struct., **51**, 4462–4476, 2014.
22. A. VASILIEV, S. VOLKOV, S. AIZIKOVICH, Y.-R. JENG, *Axisymmetric contact problems of the theory of elasticity for inhomogeneous layers*, J. Appl. Math. Mech., **94**, 705–712, 2014.
23. J. YAN, X. LI, *Double receding contact plane problem between a functionally graded layer and an elastic layer*, Eur. J. Mech. A/Solids, **53**, 143–150, 2015.
24. I. COMEZ, *Contact problem for a functionally graded layer indented by a moving punch*, Int. J. Mech. Sci., **100**, 339–344, 2015.
25. L.I. KRENEV, S.M. AIZIKOVICH, Y.V. TOKOVYY, Y.C. WANG, *Axisymmetric problem on the indentation of a hot circular punch into an arbitrarily nonhomogeneous half-space*, Int. J. Solids Struct., **59**, 18–28, 2015.
26. Z. WANG, C. YU, Q. WANG, *An efficient method for solving three-dimensional fretting contact problems involving multilayered or functionally graded materials*, Int. J. Solids Struct., **66**, 46–61, 2015.
27. R. KULCHYTSKY-ZHYHAILO, A.S. BAJKOWSKI, *Three-dimensional analytical elasticity solution for loaded functionally graded coated half-space*, Mech. Res. Commun., **65**, 43–50, 2015.
28. J. MA, S. EL-BORGI, L.L. KE, Y.S. WANG, *Frictional contact problem between a functionally graded magnetoelastoelectric layer and a rigid conducting flat punch with frictional heat generation*, J. Therm. Stresses, **39**, 245–277, 2016.
29. Y. ALINIA, A. BEHESHTI, M.A. GULER, S. EL-BORGI, A.A. POLYCARPOU, *Sliding contact analysis of functionally graded coating-substrate system*, Mech. Mater., **94**, 142–155, 2016.
30. K.S. PAREL, D.A. HILLS, *Frictional receding contact analysis of a layer on a half-plane subjected to semi-infinite surface pressure*, Int. J. Mech. Sci., **108-109**, 137–143, 2016.
31. F. ERDOGAN, G. GUPTA, *On the numerical solutions of singular integral equations*, Q. Appl. Math., **29**, 525–534, 1972.
32. A.O. CAKIRIGLU, *Elastik yarım düzleme oturan plaklarda temas problemi (Contact problem of plates resting on elastic half-plane)* Civil Engineering Department, Karadeniz Technical University, Trabzon, Turkey, 1979 [in Turkish].
33. M.B. CIVELEK, F. ERDOGAN, *Interface separation in a frictionless contact problem for an elastic layer*, J. Appl. Mech., **43**, 175–177, 1976.
34. M.B. CIVELEK, F. ERDOGAN, A.O. CAKIROGLU, *Interface separation for an elastic layer loaded by a rigid stamp*, Int. J. Engng. Sci., **16**, 669–679, 1978.

Received September 10, 2016; revised version December 1, 2016.

